Distinct Properties of CRAC and MIC Channels in RBL Cells

J. Ashot Kozak,[1] Hubert H. Kerschbaum,[1,2] and Michael D. Cahalan[1]

[1]Department of Physiology and Biophysics, University of California at Irvine, Irvine, CA 92697
[2]Department of Animal Physiology, University of Salzburg, Institute for Zoology, A-5020 Salzburg, Austria

ABSTRACT In rat basophilic leukemia (RBL) cells and Jurkat T cells, Ca^{2+} release–activated Ca^{2+} (CRAC) channels open in response to passive Ca^{2+} store depletion. Inwardly rectifying CRAC channels admit monovalent cations when external divalent ions are removed. Removal of internal Mg^{2+} exposes an outwardly rectifying current (Mg^{2+}-inhibited cation [MIC]) that also admits monovalent cations when external divalent ions are removed. Here we demonstrate that CRAC and MIC currents are separable by ion selectivity and rectification properties: by kinetics of activation and susceptibility to run-down and by pharmacological sensitivity to external Mg^{2+}, spermine, and SKF-96365. Importantly, selective run-down of MIC current allowed CRAC and MIC current to be characterized under identical ionic conditions with low internal Mg^{2+}. Removal of internal Mg^{2+} induced MIC current despite widely varying Ca^{2+} and EGTA levels, suggesting that Ca^{2+}-store depletion is not involved in activation of MIC channels. Increasing internal Mg^{2+} from submicromolar to millimolar levels decreased MIC currents without affecting rectification but did not alter CRAC current rectification or amplitudes. External Mg^{2+} and Cs^{+} carried current through MIC but not CRAC channels. SKF-96365 blocked CRAC current reversibly but inhibited MIC current irreversibly. At micromolar concentrations, both spermine and extracellular Mg^{2+} blocked monovalent MIC current reversibly but not monovalent CRAC current. The biophysical characteristics of MIC current match well with cloned and expressed TRPM7 channels. Previous results are reevaluated in terms of separate CRAC and MIC channels.

KEY WORDS: store-operated channel • CRAC channel • Ca^{2+} channel • TRPM7 • cation channel

INTRODUCTION

In T lymphocytes and rat basophilic leukemia (RBL)* cells, Ca^{2+}-release-activated Ca^{2+} (CRAC) channels play a major role in Ca^{2+} signaling and cellular activation events that lead to secretion and cell proliferation. CRAC channels, like other store-operated Ca^{2+} channels, open by an unknown mechanism when Ca^{2+} is depleted from intracellular stores (Hoth and Penner, 1992; Zweifach and Lewis, 1993). Active depletion of Ca^{2+} stores can take place by receptor stimulation to generate IP_3-induced Ca^{2+} release, by addition of thapsigargin or other SERCA pump inhibitors to inhibit Ca^{2+} sequestration, or by whole-cell recording with addition of IP_3 to the pipette solution. In a passive depletion paradigm, CRAC channels are activated during whole-cell recording within 1–3 min simply by dialyzing the cytoplasm with a high concentration of Ca^{2+} chelator, either EGTA or BAPTA. Ca^{2+} ions that passively leak from intracellular stores are rapidly bound, thereby depleting the Ca^{2+} stores and resulting in CRAC channel activation (Lewis and Cahalan, 1989; Zweifach and Lewis, 1993).

CRAC channels, like voltage-activated Ca^{2+} channels (Hess and Tsien, 1984; Almers and McCleskey, 1984) and several other cation channels, are selective for Ca^{2+} ions in physiological solutions and conduct monovalent cations when external divalent ions are removed (Hoth and Penner, 1993; Premack et al., 1994). Within the series of alkali metal cations, Li^{+}, Na^{+}, K^{+}, and Rb^{+} are equally permeant but Cs^{+} is only sparingly permeant through CRAC channels (Lepple-Wienhues and Cahalan, 1996). Monovalent current through CRAC channels retains the property of inward rectification seen with divalent ions. Upon removal of external divalent ions the monovalent current inactivates (also termed depotentiation; Zweifach and Lewis, 1996) within tens of seconds. All studies described above were performed with 1–3 mM internal free [Mg^{2+}].

Omission of external and internal divalent ions led to a much larger monovalent current in Jurkat T cells, with properties that were similar but not identical to monovalent current through CRAC channels recorded with internal Mg^{2+} present (Kerschbaum and Cahalan, 1998). In contrast to CRAC channels, the monovalent current did not inactivate, had a nearly linear I-V characteristic, and conducted Cs^{+} just as well as Na^{+}. During whole-cell recording from Jurkat and normal human T cells, 40-pS single channels with high open probability were seen during activation, inactivation, and run-down (Kerschbaum and Cahalan, 1999; Fomina et al., 2000). Under identical conditions, a similar current develops in RBL

Address correspondence to Michael D. Cahalan, Department of Physiology and Biophysics, University of California, Irvine, CA 92697-4561. Fax: 949-824-3143; E-mail: mcahalan@uci.edu

*Abbreviations used in this paper: CRAC, Ca^{2+}-release-activated Ca^{2+}; IRK, inwardly rectifying K^{+}; MIC, Mg^{2+}-inhibited cation; RBL, rat basophilic leukemia.

J. Gen. Physiol. © The Rockefeller University Press • 0022-1295/2002/08/221/15 $5.00
Volume 120 August 2002 221–235
http://www.jgp.org/cgi/doi/10.1085/jgp.20028601

cells and exhibits similar single-channel characteristics (Braun et al., 2001). These single channels were proposed to represent CRAC channels with properties modulated by Mg^{2+} removal (modulated CRAC hypothesis). However, the alternative possibility remained that a different type of cation channel was revealed by the simultaneous removal of Mg^{2+} from the cytoplasm and divalent ions from the bath (two-channel hypothesis). The difficulty of distinguishing between these two hypotheses was compounded by a lack of molecular information on CRAC channels and a corresponding lack of information on the mechanism of store-dependent activation and monovalent-current inactivation. However, the cloning and expression of TRPM7 (Nadler et al., 2001; Runnels et al., 2001), with properties that include outward rectification and inhibition by internal Mg^{2+}, force a reexamination of the modulated CRAC hypothesis. TRPM7, a novel TRP gene formerly named ChaK, TRPPLIK, or LTRPC7 contains both channel and kinase sequence motifs and displays outwardly rectifying cation currents when expressed in mammalian cells, with properties similar to native currents recorded with low internal Mg^{2+} (or Mg^{2+}-ATP) in RBL and Jurkat T cells. The outwardly rectifying native currents that develop when Mg^{2+} and Mg^{2+}-ATP are omitted have been called magnesium-nucleotide–regulated metal cation current (MagNuM) (Hermosura et al., 2002) and Mg^{2+}-inhibited cation current (MIC) (Prakriya and Lewis, 2002); here we adopt the latter terminology.

Recent studies suggest that separate and independent CRAC and MIC channels provide the most parsimonious explanation of differences between currents in the presence and absence of internal Mg^{2+} (Hermosura et al., 2002; Prakriya and Lewis, 2002). Our results complement and extend these studies by providing additional ways to distinguish and separate the current components based on differences in ion permeation, pharmacological sensitivities, and susceptibility to run-down. We exploit selective run-down of MIC to compare and contrast properties of CRAC and MIC channels under identical ionic conditions with low internal Mg^{2+}. We discuss and reinterpret previous studies on Jurkat and human T cells (Kerschbaum and Cahalan, 1998, 1999; Fomina et al., 2000) in terms of separate MIC and CRAC currents, each capable of mediating Ca^{2+} influx. Some of the data presented in this article have appeared previously in abstract form (Kozak and Cahalan, 2001, 2002).

MATERIALS AND METHODS

Cell Culture

RBL-2H3 cells (Siraganian et al., 1982) were cultured in Eagle's MEM supplemented with 10% fetal bovine serum in 5% CO_2-humidified atmosphere at 37°C. Cells were passaged twice weekly and plated on glass coverslips for recording (McCloskey and Cahalan, 1990).

Patch-Clamp Recording

Whole-cell recordings were done on RBL cells 1–3 d after plating, using an EPC-9 patch clamp amplifier (HEKA Elektronik). Patch pipettes were fabricated from soda lime glass capillaries (Becton Dickinson and Kimble) on a DMZ-Universal Puller (Zeitz) and coated with sylgard (Dow Corning Corp.) near the tips. The resistances of fire-polished pipettes were 1.5–4 MΩ when filled with K^+ or Cs^+ glutamate–containing solutions. Fast and slow capacitance transients were compensated using the EPC-9 circuitry. Voltage ramps (−120 to 70 mV or −120 to 85 mV, 211-ms duration) were delivered at 0.5 Hz to obtain current-voltage relations. The holding potential between the ramps was 0 mV. Data were analyzed using Pulse/Pulsefit, v. 8.11 (HEKA Elektronik), Igor Pro (v. 3.1.2) (WaveMetrics), and Microcal Origin (v. 6) (Microcal Software) software. To determine the reversal potential of the current induced by dialysis, we subtracted I-V traces after complete run-down from I-V traces collected at the peak of current development (usually around 10 min after break-in) to correct for a small leakage current that did not vary significantly in good experiments. Experiments were conducted at room temperature.

The "high EGTA" internal solution contained (mM): 130 Cs^+ glutamate, 8 NaCl, 0.9 $CaCl_2$, 12 EGTA, 10 HEPES, pH 7.3 titrated with CsOH. When necessary, 0.15–5 mM $MgCl_2$ was added to this solution yielding free Mg^{2+} concentrations of ~83 μM to 3 mM as estimated by Maxchelator (v. 1.78) software (written by Chris Patton, Stanford University). The "low EGTA" internal solution contained (mM) 150 K^+ or Cs^+ glutamate, 1 EGTA, 0.5 $CaCl_2$, 10 HEPES, pH 7.3 titrated with K^+ or CsOH. Free Ca^{2+} concentration in high and low EGTA internal solution was ~9 nM and ~92 nM, respectively, as estimated by Maxchelator. In some experiments, internal 12 mM EDTA with higher affinity for Mg^{2+} than EGTA was used in order to remove cytosolic Mg^{2+} more completely. Divalent-free external solution, referred to as "Na^+–HEDTA," contained (mM): 154 Na^+ aspartate, 5 NaCl, 10 HEDTA, 10 HEPES, pH 7.3 titrated with NaOH. Li^+, Cs^+, or NH_4^+ were substituted for Na^+ in one series of experiments. Divalent-containing external solutions contained (mM): 2–5 $CaCl_2$ or $MgCl_2$, 10 HEPES, 167 Na^+ aspartate, pH 7.3 titrated with NaOH. Aspartate and glutamate were used as the main anions in internal and external solutions to minimize Cl^- currents. In most experiments, 2 Cs^+ methanesulfonate was added to block native inward rectifier K^+ currents (Wischmeyer et al., 1995). Experiments testing the effect of increased internal Ca^{2+} on MIC activation parameters and comparing MIC and inward rectifier K^+ current development time course were performed in external solution containing (mM): 4.5 KCl, 2 Ca^{2+}, 1 Mg^{2+}.

Spermine (hydrochloride) stock (5 mM) was prepared in divalent-free external solution and stored at 4°C. SKF-96365 (hydrochloride) (1-[b-[3-(4-methoxyphenyl)propoxy]-4-methoxyphenethyl]-1H-imidazole, HCl) and thapsigargin stock solutions were prepared in DMSO and kept frozen. After diluting in external solutions the final DMSO concentration was below 0.1%. Spermine, SKF-96365, and thapsigargin were from Calbiochem. All other chemicals were purchased from Sigma-Aldrich.

RESULTS

Removal of internal Mg^{2+} changes the rectification and ion permeability characteristics of cation currents in RBL and Jurkat cells (Kerschbaum and Cahalan, 1998;

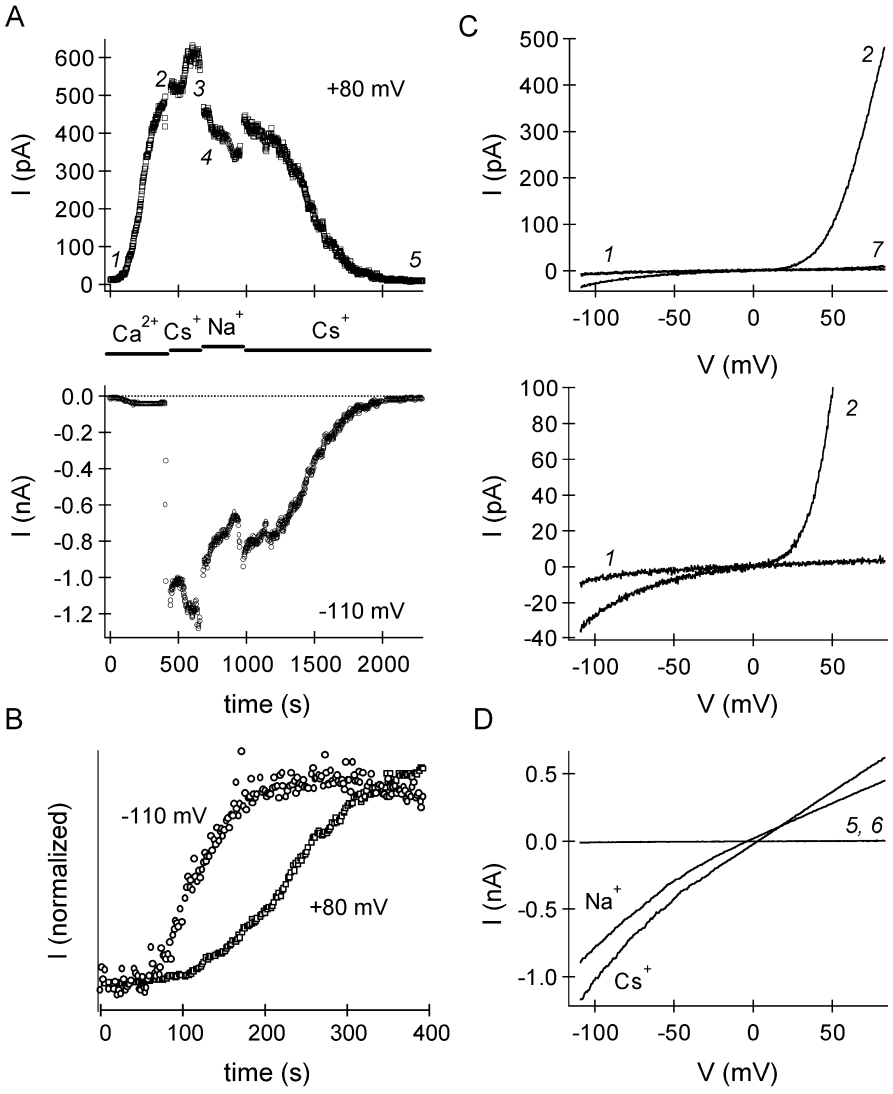

FIGURE 1. Development and run-down of CRAC and MIC currents in the presence and absence of external divalent ions. Internal solution contained 12 mM EGTA and no added Mg^{2+}. (A) Outward (top) and inward (bottom) current development in 2 mM external Ca^{2+}, followed at ~400 s by exposure to Cs^+– then Na^+–HEDTA. MIC ran down gradually over 2,000 s. (B) Current development time course for inward and outward currents compared. The scaled and inverted inward current measured at −110 mV is shown superimposed with the outward current (80 mV). The inward current clearly precedes the development of the outward current, despite its smaller size. (C) I-V plots of MIC current in 2 mM Ca^{2+} plotted with two different current amplitude scales. Traces 1 and 2 correspond to times indicated in A. Trace 7 was collected 51 min after break-in after reintroduction of 2 mM Ca^{2+}. (D) I-V plots of monovalent MIC current in Na^+– and Cs^+–HEDTA. Both Cs^+ and Na^+ are permeant through the channel. The indistinguishable traces 5 and 6 (taken 54 min after break-in) were obtained in Cs^+ and Na^+ solution, respectively, after complete run-down of MIC current.

Nadler et al., 2001; Hermosura et al., 2002; Prakriya and Lewis, 2002). Operationally, the additional current that develops as cytoplasmic [Mg^{2+}] is lowered can be defined as the MIC component of current. Fig. 1 outlines the general characteristics of currents activated by dialysis with a pipette solution containing high EGTA to deplete Ca^{2+} stores passively while lowering internal Mg^{2+}. Two components of current are present in this experiment but overlap kinetically. Within minutes after break-in, large outward currents carried by Cs^+ and much smaller inward currents developed in external solution containing 2 mM Ca^{2+} (Fig. 1 A). The removal of external divalent ions (using a divalent-free solution with 10 mM HEDTA) increased the amplitude of inward currents with only minor change in the outward Cs^+ current at 80 mV. Both Na^+ and Cs^+ carried inward current in divalent-free external solution. On expanded time and current amplitude scales, the inward current can be seen to activate somewhat more rapidly than the outward current at the beginning of the experiment, suggesting the presence of more than one type of channel or, alternatively, the evolution of I-V characteristics of a single type of channel (Fig. 1 B). Current-voltage relations before, during, and after current development illustrate strong outward rectification of the induced current in the presence of external Ca^{2+} (Fig. 1 C). When Ca^{2+} was withdrawn, the I-V curves in Na^+ and Cs^+ revealed slight inward rectification (Fig. 1 D). After reaching a peak, the inward and outward currents declined to zero after ~2,000 s. Our goal is to test whether reducing internal Mg^{2+} modulates CRAC channel properties or reveals a second population of outwardly rectifying MIC channels.

Properties of MIC Current

Divalent and monovalent ion permeation. One of the hallmarks of the CRAC current is its positive reversal potential in physiological levels of external Ca^{2+}. Reversal po-

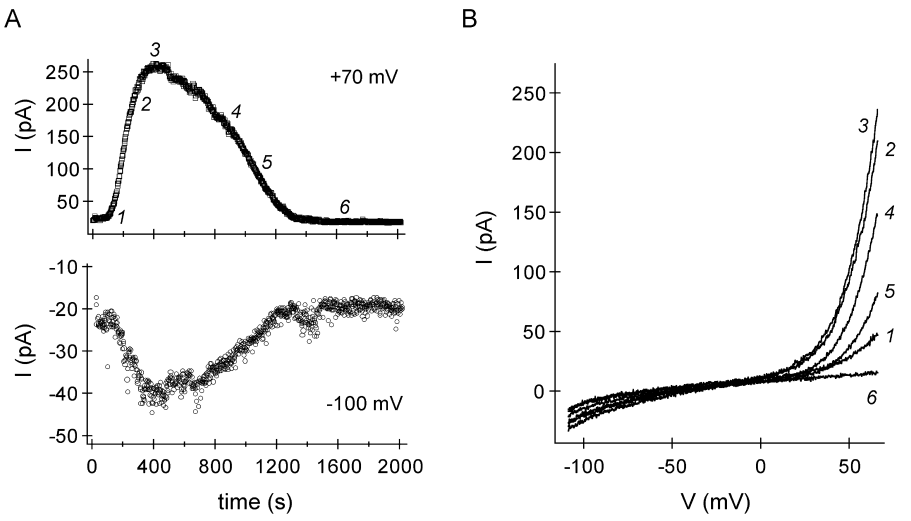

FIGURE 2. MIC current is permeable to external Mg^{2+}. Internal solution contained 12 mM EGTA and no added Mg^{2+}. External solution contained 2 mM Mg^{2+} and Na^+ aspartate. (A) MIC-current development and run-down in 2 mM external Mg^{2+} with zero Ca^{2+}. (B) I-V relations of MIC current in 2 mM Mg^{2+} obtained at various times after break-in (same cell as in A).

tentials of the induced current were close to 0 mV (Fig. 1 C, shown with two current scales in C) when the external medium contained 2 mM Ca^{2+}. Significantly, the reversal potential was also close to 0 mV when the external solution contained only Mg^{2+}, Ca^{2+}, Na^+, or Cs^+ as the major external permeant ion, with Cs^+ inside. Differences in reversal potential and permeant ions distinguish a larger component of MIC current from the smaller CRAC current. The current in external Cs^+ usually reversed at slightly more positive potentials than in Na^+ (Fig. 1 D), indicating that Cs^+ is slightly more permeant through this channel than Na^+. By reversal potential measurement, the following cations had the relative permeability sequence: NH_4^+ (1.3) > Cs^+ (1.1) > Li^+ (1.0) ~ Na^+ (1.0 by definition). Among larger monovalent cation substitutes, $NMDG^+$ was not measurably permeant and tetramethylammonium was sparingly permeant (unpublished data). These results are consistent with previous data (Kerschbaum and Cahalan, 1998), but with the revision that these properties are characteristic of the MIC component of current, not CRAC.

TRPM7 channels expressed in HEK cells are reportedly permeable to Mg^{2+} in the absence of Ca^{2+}, based on the presence of inward current in isotonic Mg^{2+} solution (Nadler et al., 2001). Since MIC currents in native Jurkat and RBL cells resemble TRPM7 in the expression system, we examined whether Mg^{2+} current can be detected using physiological levels of Mg^{2+} in RBL cells dialyzed with 12 mM EGTA and no added Mg^{2+}. With 2 mM external Mg^{2+} present and Ca^{2+} absent, an inward current developed and ran down in parallel with the outward current during dialysis with zero internal Mg^{2+} (Fig. 2), consistent with Mg^{2+} current through the MIC channel. Fig. 2 B illustrates I-V curves recorded at different time points of current development. At negative potentials, the inward current did not consistently increase when Mg^{2+} concentration was varied from 2 to 5 mM. However, by process of elimination, Mg^{2+} is the main current-carrying ion, because inward current was still observed in the absence of external Na^+ (substituted by the impermeant cation $NMDG^+$), leaving Mg^{2+} as the only remaining cation. Substituting internal HEPES by TRIS also did not affect the inward current with external Mg^{2+} ($n = 3$ cells). At positive potentials, the current was outward, conducting Cs^+ from the inside. I-V shapes were similar with 2 mM external Mg^{2+} or Ca^{2+}, although currents were markedly and uniformly reduced at all potentials with external Mg^{2+} as the only divalent ion. We conclude that the MIC current discriminates poorly among monovalent cations (in the absence of divalent ions) as well as between Ca^{2+} and Mg^{2+}. The ability of Mg^{2+} and Cs^+ to carry inward current is characteristic of the MIC, but not the CRAC component of current.

MIC I-V Shape Is Mg^{2+}- and Time-invariant

Internal Mg^{2+} greater than ~3 mM inhibited MIC current completely, in agreement with Nadler et al. (2001). If Mg^{2+} inhibition were mediated by a direct interaction with the conducting pore, intermediate levels of Mg^{2+} might alter I-V shape as a result of voltage-dependent block, as is seen in several types of ion channels interacting with Mg^{2+}, including inwardly rectifying K^+ channels, nicotinic acetylcholine receptor channels, L-type Ca^{2+} channels, and voltage-gated Na^+ channels (Matsuda et al., 1987; Vandenberg, 1987; Pusch, 1990; Ifune and Steinbach, 1992; Kuo and Hess, 1993; Nichols et al., 1994; Forster and Bertrand, 1995). However, at different internal free Mg^{2+} levels from subnanomolar (zero added Mg^{2+} with 12 mM EDTA) to 1.15 mM, the shape of the MIC I-V curve remained constant although current magnitudes varied widely, both in the presence or absence of external divalent ions (Fig. 3). When the pipette solution contained zero

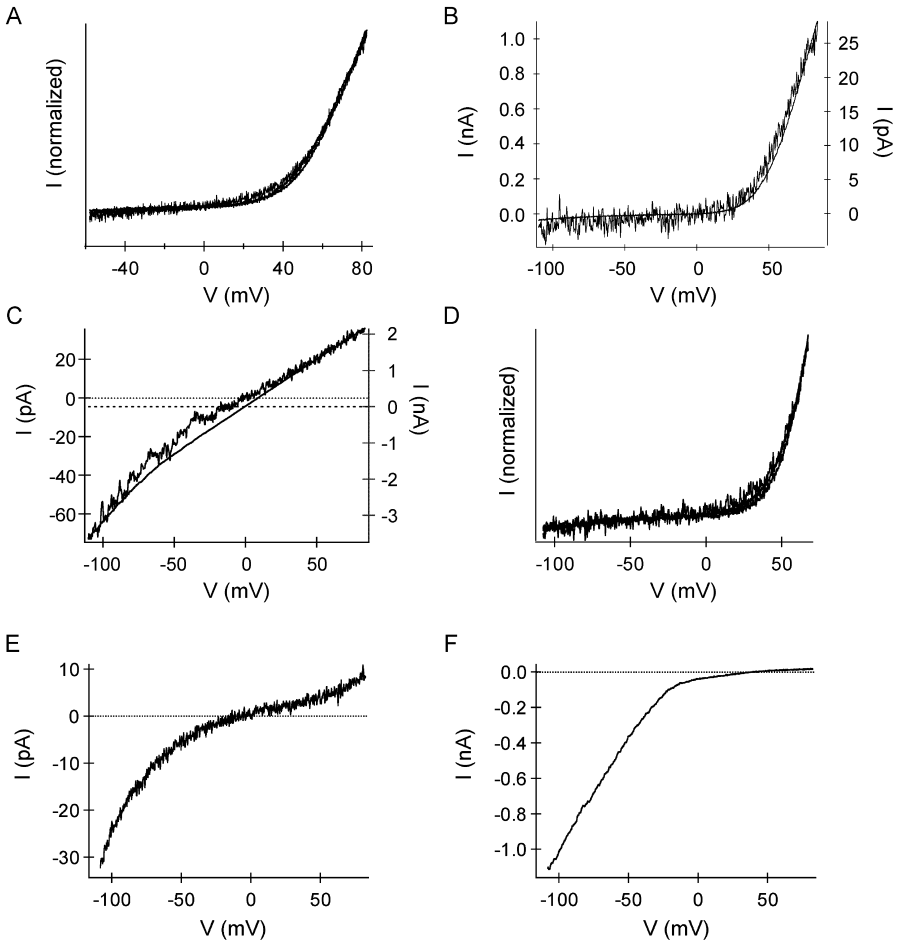

FIGURE 3. MIC I-V shape does not depend on internal [Mg^{2+}] or dialysis time after break-in. (A) Scaled and superimposed MIC I-V relations from three different cells with 0, 0.5, and 1 mM Mg^{2+} in pipette. Free [Mg^{2+}] concentrations were estimated by calculation with Maxchelator: nominally zero, ~280 μM, and ~563 μM. External solution contained 2 mM Ca^{2+}. (B) MIC current I-V from two different cells with 0 and 2 mM Mg^{2+} in the pipette with 2 mM external Ca^{2+}. Note the different current axis scales, with the smaller, noisy current trace (2 mM internal Mg^{2+}) corresponding to the pA scale. The internal solutions contained (mM): 12 EDTA + 0 Mg^{2+} (nominally Mg^{2+}-free); and 12 EGTA + 2 total (~1.15 free) Mg^{2+}. (C) MIC I-V in the absence of external divalent ions, with 0 and 2 mM Mg^{2+} in the pipette as in B. External solution: Cs^+–HEDTA to minimize CRAC current contamination (see Fig. 9). (D) Superimposed scaled traces from Fig. 2 B in 2 mM external Mg^{2+} at varying times following break-in, showing that the I-V characteristic of MIC current is time-invariant. Mg^{2+} was used as the permeant ion to minimize possible contamination by CRAC current. Internal solution: 12 mM EGTA, 0 Mg^{2+}. (E and F) MIC current recorded with internal $NMDG^+$ as the predominant cation. I-V curves in 2 mM Ca^{2+} and Na^+–HEDTA, respectively. The low-EGTA internal solution contained $NMDG^+$ as an impermeant cation substitute. External solutions were 2 mM Ca^{2+} (E) and Na^+–HEDTA (F).

added Mg^{2+}, the I-V relation showed strong outward rectification in the presence of either Ca^{2+} or Mg^{2+} (Fig. 3 A). Fig. 3, B and C, shows scaled, superimposed I-V curves with Ca^{2+} carrying the inward current and almost linear I-V relations with Cs^+ carrying the inward current in the absence of external divalent ions. Internal Mg^{2+} reduced current magnitudes uniformly at all potentials. We also tested whether the MIC I-V shape is stationary during whole-cell recording as internal Mg^{2+} is washed out during dialysis of cytoplasm by the pipette contents. During development and run-down of MIC current, the I-V shape remained constant, shown by superimposing scaled I-V curves at varying times after break-in (Fig. 3 D). In Fig. 3, E and F, the outward current did not develop when $NMDG^+$ was the sole cation in the pipette. After ~10 min of dialysis the external solution was switched from 2 mM Ca^{2+} to Na^+–HEDTA and the inward current became visible. Thus, it is possible for the MIC I-V to be inwardly rectifying when internal permeant ions are eliminated but not when internal Mg^{2+} is increased. The MIC I-V shape appears to be intrinsic to the channel and is not tailored by dialyzable cytoplasmic constituents other than permeant monovalent cations.

Internal and External Mg^{2+} Inhibition Compared

To address the mechanism of internal Mg^{2+} inhibition, we took advantage of the observation that a small percentage of RBL cells (~5%) show a substantial MIC current upon break-in. With Mg^{2+} omitted from the pipette solution the current increased until a maximum was reached after several minutes. When the pipette contained millimolar levels of Mg^{2+}, the MIC current gradually declined, also with a slow time course. Fig. 4 A shows a recording from a cell with preactivated MIC current with 5 mM Mg^{2+} internal solution. The current was completely inhibited after ~9 min; $t_{1/2}$ averaged 117 ± 41 s, $n = 7$ cells. The time course of internal Mg^{2+} inhibition is too slow for direct channel block by Mg^{2+}, since complete dialysis of the cell cytoplasm by Mg^{2+} is complete within <1 min (Pusch and Neher, 1988). In contrast, block of mono-

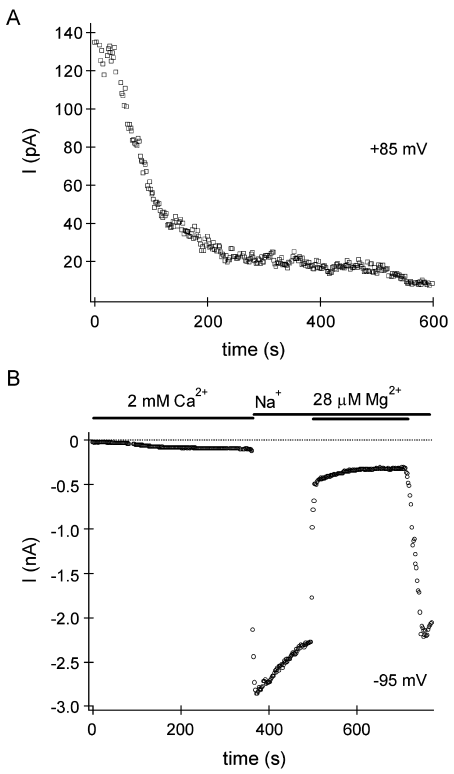

FIGURE 4. Effects of external and internal Mg^{2+} on MIC current. (A) Time course of internal Mg^{2+} inhibition of preactivated MIC current. The pipette solution contained: 12 mM EGTA, 5 mM total (~3 mM free) Mg^{2+}. Outward current amplitude was measured at 85 mV, and the half-time of inhibition was 85 s. (B) Time course of external Mg^{2+} inhibition of MIC current. The pipette solution contained: 12 mM EGTA, 0 Mg^{2+}. MIC current developed first in 2 mM Ca^{2+} external. Monovalent MIC current in Na^+–HEDTA was blocked reversibly by 28 μM external Mg^{2+} (8 mM HEDTA + 3 mM $MgCl_2$).

valent current by external Mg^{2+} is fast and voltage-dependent, indicating a high-affinity binding site for Mg^{2+} within the pore (Fig. 4 B).

Ca^{2+} Buffering Does Not Affect the Size or the Time Course of MIC Current Development

To determine whether store depletion is necessary to evoke the MIC current, we tested conditions that would be expected to alter store content. One approach to address this question is to increase internal free Ca^{2+} concentration, thus reducing the Ca^{2+} gradient between the intracellular store and the cytoplasm. In a paired comparison trial, the MIC current was recorded with low EGTA (1 mM) with ($n = 7$ cells) or without ($n = 14$ cells) 0.5 mM Ca^{2+} (~90 nM free) in the pipette. Neither the MIC current amplitude nor the rate of activation was reduced by inclusion of Ca^{2+}; if anything these parameters were increased, contrary to expectations for a store-operated channel. MIC current amplitudes normalized to cell capacitance were 5.5 ± 1.6 pA/pF in Ca^{2+}-free compared with 13.1± 2.8 pA/pF in 0.5 mM Ca^{2+}, respectively (evaluated at 70 mV, 6 min after break-in); times to maximal current were 854 ± 110 and 577 ± 55 s, respectively. Furthermore, complete omission of chelators from the pipette solution (with 10 or 100 μM Ca^{2+} added) did not prevent the activation of MIC current either (unpublished data). Conditions that suppress CRAC channel activation do not alter development of MIC current when Mg^{2+} is withdrawn from the cytoplasm.

Run-down of MIC and IRK Currents

In addition to CRAC and MIC, RBL cells express inwardly rectifying K^+ (IRK) channels thought to be Kir2.1. IRK currents run down spontaneously after prolonged dialysis (McCloskey and Cahalan, 1990; Wischmeyer et al., 1995). MIC and IRK conductances change in parallel during prolonged dialysis, first increasing to a maximum at a similar time and then running down (Fig. 5, A and B). Since IRK is a strong inward rectifier and MIC rectifies strongly in the outward direction, cross-contamination of currents is minimal at very positive and negative membrane potentials (Fig. 5 C). Contamination by CRAC channels at negative potentials is minimal due to the substantially larger IRK current magnitude. MIC and IRK run-down kinetics were highly variable from cell to cell but strongly correlated in an individual cell (n = 12 cells). It is likely that the mechanisms that govern IRK and MIC run-down are both related to PIP_2 depletion in the cell membrane (Huang et al., 1998; Rohacs et al., 1999; Runnels et al., 2002). In contrast, as we document further below, CRAC current is relatively resistant to run-down and can be characterized in isolation of other current components under conditions of low internal Mg^{2+}.

MIC Current Is Blocked by External Spermine

External Mg^{2+} in the micromolar range blocks monovalent MIC current in a voltage-dependent manner (Fig. 4 B). Polyamines also block several other channel types that display open channel Mg^{2+} block, including IRK channels and AMPA glutamate receptors (for review see Williams, 1997), nAChRs (Haghighi and Cooper, 2000), cyclic nucleotide–gated channels (Lu and Ding, 1999), and voltage-gated Na^+ channels (Huang and Moczydlowski, 2001). Fig. 6 A shows that MIC currents carried by Cs^+ in the absence of external divalent ions are blocked by spermine at micromolar concentrations. The dose–response relation for spermine block of Cs^+ current (Fig. 6 B) indicates a K_d value of 2.3 μM at −100 mV. Like external Mg^{2+} block, spermine block was fast and voltage dependent, with relief of block at both depolarized and hyperpolarized potentials, indicating interaction with a site within the conducting

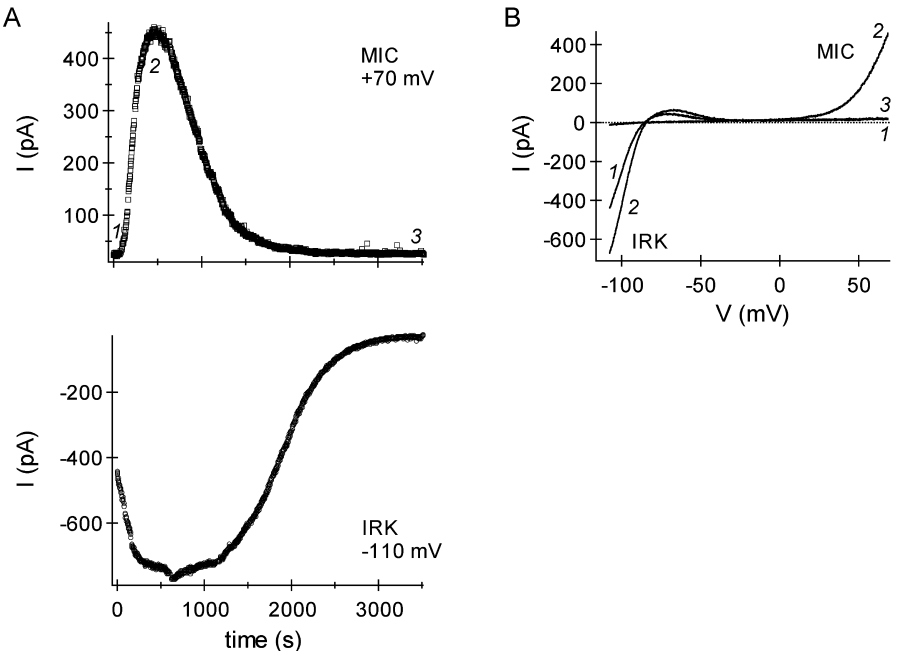

FIGURE 5. MIC and the endogenous IRK currents activate and run down in parallel. (A) Time course of development of MIC current measured at 70 mV and IRK current measured at −110 mV. (B) I-V shapes at various times. IRK was preactivated at break-in, whereas MIC was absent. The internal solution contained (mM): K^+ glutamate, 1 EGTA, 0.5 Ca^{2+}, 0 Mg^{2+}. The external solution contained (mM) 4.5 KCl, 2 Ca^{2+}, 1 Mg^{2+}.

pore and punch through at very negative potentials. Spermine provides a pharmacological tool to test for monovalent MIC current.

SKF-96365 Accelerates Run-down of MIC Current

SKF-96365 (Merritt et al., 1990; Chung et al., 1994) has been shown to block CRAC current reversibly at 10–20 μM (IC_{50} values vary from 11 to 16 μM). We investigated effects of 20 μM SKF applied after complete development of MIC current (Fig. 7). SKF inhibits MIC with slow onset kinetics that are consistent with an indirect action rather than direct channel blockade. Indeed, SKF (20 μM) had very little effect on the MIC channels in human T cells (unpublished data). The time course of SKF inhibition was variable from cell to cell. Interestingly, SKF exposure seemed to prime the currents for run-down; MIC currents continued to decrease at the same rate even after SKF was washed out. SKF inhibition was entirely irreversible. Pretreatment of intact RBL cells with SKF did not prevent the subsequent development of MIC, but SKF still exerted its inhibitory effect when reapplied. SKF also inhibited the monovalent current through MIC channels in divalent-free conditions. As a working hypothesis, we propose that SKF acts to facilitate the run-down process through an unknown mechanism that may involve accelerated PIP_2 depletion. Consistent with this hypothesis, in preliminary experiments SKF also facilitated the run-down of IRK current. Since the speed of drug action varied from cell to cell, with no effect in a minority of cells, SKF inhibition of MIC current is not a simple and direct blocking action.

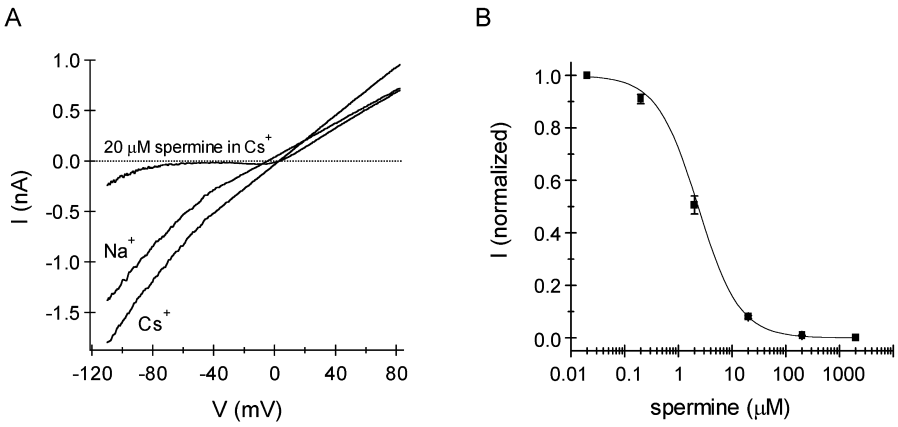

FIGURE 6. Extracellular spermine blocks the MIC current in divalent-free solution. (A) 20 μM spermine was applied externally after MIC current had developed fully in divalent-free solution (Na^+–and Cs^+–HEDTA). Block was strongly voltage-dependent, blocking preferentially the inward current, but showing some relief of block at very negative potentials. Internal solution: 12 mM EGTA, 0 Mg^{2+}. Spermine block was completely reversible (not shown). (B) Dose-response relationship for spermine block of Cs^+ current (to minimize possible CRAC current contamination) at −100 mV. Data from nine cells are fitted with the Hill equation using a K_d value of 2.3 μM and a Hill coefficient of 1.1.

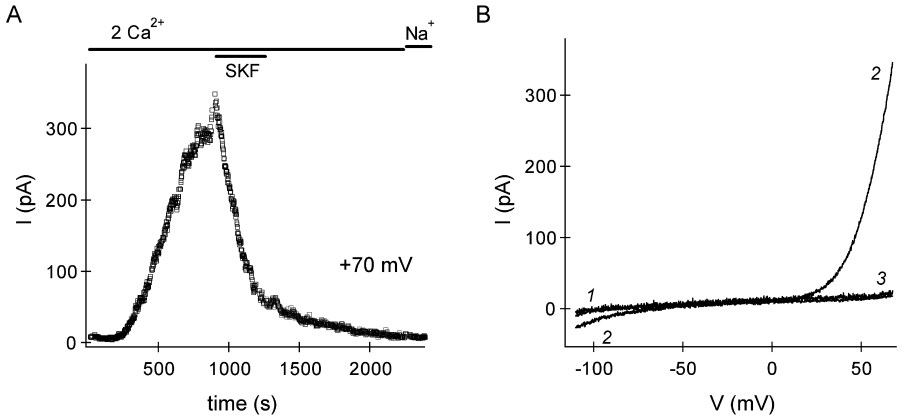

FIGURE 7. SKF-96365 irreversibly inhibits MIC current. (A) 20 μM SKF was applied after development of MIC current in 2 mM Ca^{2+}. (B) I-V relations in a different cell after break-in (*1*), after development of MIC current (*2*), and after SKF inhibition (*3*). Internal solution contained 2 mM EGTA.

Properties of CRAC Current

Divalent and monovalent permeation. To investigate CRAC channels in isolation, 6 mM internal Mg^{2+} (free [Mg^{2+}] = 3.67 mM) was used to prevent activation of MIC channels (Fig. 8). In Ca^{2+}-free external solution (with 2 mM Mg^{2+}) the characteristic development of inward CRAC current was not seen, because Mg^{2+} is impermeant. Nevertheless, CRAC channels were activated, because inward current was immediately detected upon switching the external solution to 2 mM Ca^{2+} (with 0 Mg^{2+}). Subsequently, after removal of all external divalent ions, an inactivating Na^+ current was seen, and this current was greatly reduced in external Cs^+, confirming previous observations in Jurkat cells that CRAC channels do not conduct Cs^+ well (Lepple-Wienhues and Cahalan, 1996). Fig. 8 B shows corresponding I-V curves in the presence and absence of external Ca^{2+} and Mg^{2+}. In Ca^{2+}, the current was inwardly rectifying, whereas in Mg^{2+} inward currents were reduced and only a linear leak current was observed. Monovalent CRAC I-V curves in Na^+ and Cs^+ show that Na^+, but not Cs^+, permeates readily and displays the same degree of inward rectification as Ca^{2+} current (Fig. 8 C). These results confirm that CRAC channels are highly selective for Ca^{2+} over Mg^{2+} and, upon removal of divalents, Na^+ over Cs^+ (Hoth and Penner, 1993; Lepple-Wienhues and Cahalan, 1996).

Varying Internal Mg^{2+} Does Not Affect the I-V Shape of CRAC Channels

Fig. 9 A shows CRAC current with 5 mM internal [Mg^{2+}], corresponding to ~3 mM free [Mg^{2+}]. At this level of internal Mg^{2+}, the MIC current was very small, and only CRAC current was observed. With 2 mM external Ca^{2+}, the I-V of CRAC current was inwardly rectifying as ex-

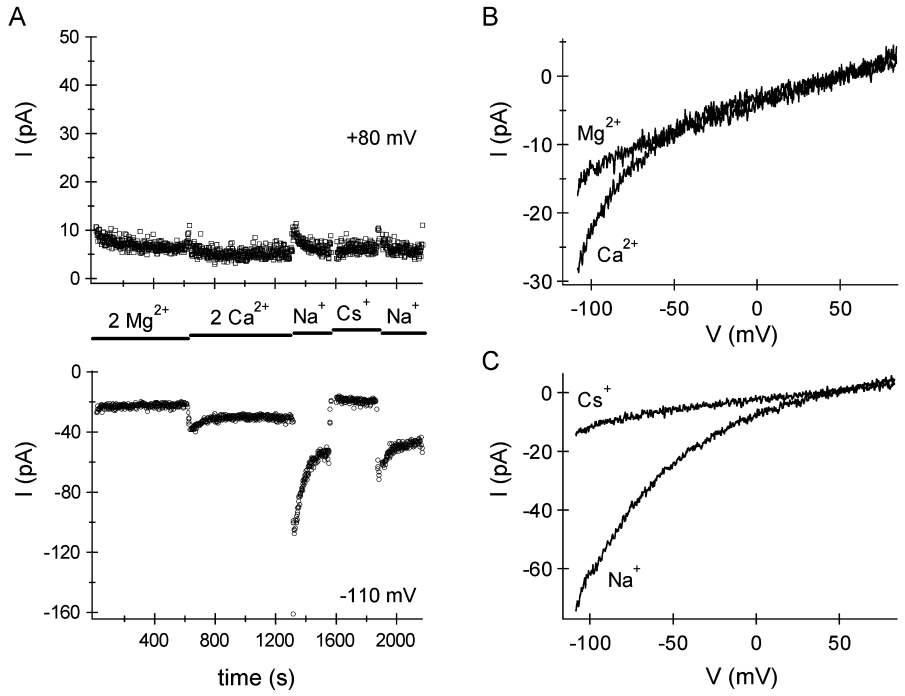

FIGURE 8. Divalent and monovalent selectivity of CRAC channels. Internal solution contained 12 mM EGTA, with 6 mM total (~3.67 free) Mg^{2+} to block MIC current development. (A) Time course of inward and outward currents showing inward CRAC Ca^{2+} and monovalent currents. Recording was started in 2 mM Mg^{2+}; the time-dependent activation of Mg^{2+} MIC current was absent. Adding 2 mM Ca^{2+} revealed CRAC current. The inward monovalent current showed partial inactivation in Na^+ - HEDTA, and was greatly reduced in Cs^+ - HEDTA. (B) I-V curves in 2 mM external Mg^{2+} and Ca^{2+}. (C) I-V curves in Na^+ - and Cs^+ - HEDTA.

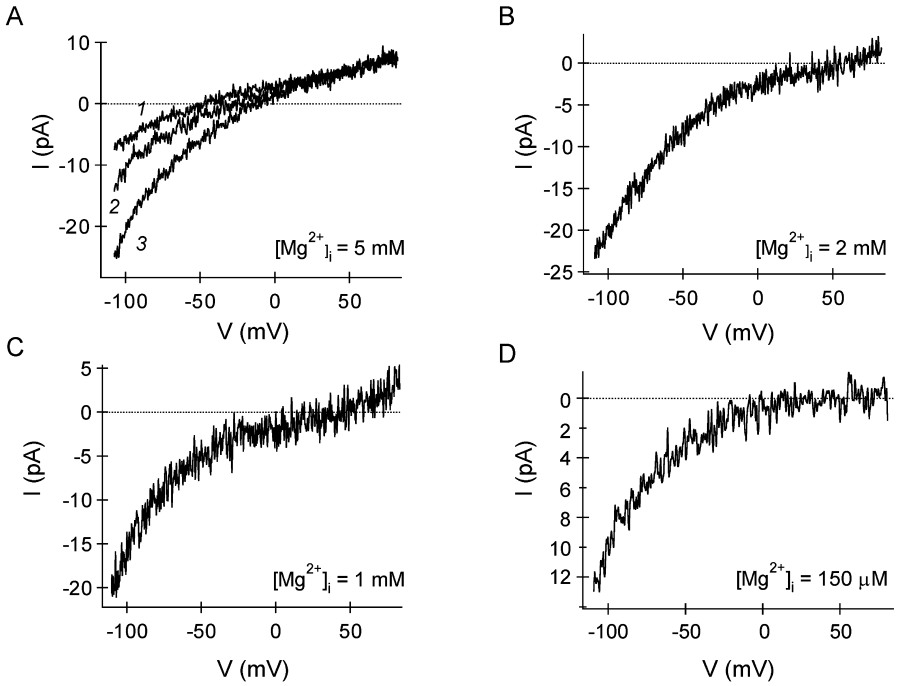

FIGURE 9. CRAC current inward rectification is independent of internal Mg^{2+}. All pipette solutions contained 12 mM EGTA. (A) Trace *1* shows current after break-in. Traces *2* and *3* show CRAC current in 2 and 5 mM external Ca^{2+}. Internal solution: 5 mM total (~3 mM free) Mg^{2+}. The current is strongly inwardly rectifying and shows no outward current at 80 mV, indicating that 3 mM free Mg^{2+} is sufficient to inhibit MIC current completely. The reversal potential is above 40 mV. Note the difference in the I-V shape compared with Fig. 1 C. (B) CRAC current in 2 mM external Ca^{2+}. Internal solution contained 2 mM total (~1.15 free) Mg^{2+}. (C) CRAC current in 5 mM external Ca^{2+} with 1 mM (~563 μM free) Mg^{2+} in pipette. (D) CRAC current in 5 mM external Ca^{2+} with 150 μM (~83 μM free) Mg^{2+} in pipette. Traces shown in B–D were obtained after run-down of MIC current.

pected with a reversal potential more positive than 40 mV (compare Hoth and Penner, 1993). Increasing external Ca^{2+} from 2 to 5 mM increased the size of the inward CRAC current, also as expected. At lower internal Mg^{2+} levels, mixtures of CRAC and a much larger MIC current component were typically observed, but CRAC current persisted after MIC current ran down completely. Fig. 9, B–D, shows a comparison of CRAC I-V shapes when internal Mg^{2+} was lowered to 2, 1, and 0.15 mM Mg^{2+}, corresponding to calculated free [Mg^{2+}] levels of 1.15–0.083 mM. The CRAC I-V relationship retained the same degree of inward rectification. By taking advantage of the selective run-down of MIC current, we show that the CRAC I-V shape does not depend upon internal [Mg^{2+}].

Pharmacological Properties of Monovalent Current through CRAC Channels

We tested the effects of external spermine and SKF-96365 on monovalent CRAC current to compare the pharmacological properties of CRAC and MIC currents. This section demonstrates that spermine had no effect on monovalent or divalent CRAC current, although it reversibly blocked monovalent MIC current (Fig. 6). In addition, SKF-96365 (20 μM) inhibited monovalent CRAC current reversibly (Fig. 10 A), as was shown previously for Ca^{2+} current through CRAC channels (Chung et al., 1994), although it inhibited MIC current irreversibly (Fig. 7). SKF-96365 block was reversible ($n = 4$) and did not show apparent voltage dependence. As shown in Fig. 10 B, 20 μM spermine failed to block Na^+ current through CRAC channels. Like spermine, external Mg^{2+} also did not affect CRAC channels at a concentration of external Mg^{2+} (28 μM free) that almost completely blocked MIC channels (Fig. 10 B, c.f. Fig. 4 B).

Separation of CRAC and MIC Currents by SKF-facilitated Run-down: Changes in Relative Na^+ and Cs^+ Permeability

SKF accelerates run-down of MIC current but blocks CRAC current reversibly. This difference was exploited to separate MIC and CRAC components under identical ionic conditions with low internal Mg^{2+}. In Fig. 11 A, both CRAC and MIC currents developed in the presence of 2 and 5 mM external Ca^{2+}. Application of SKF reduced the outward MIC current to zero within several minutes and also reduced the inward current at the same time. Inward but not outward currents recovered upon washout of SKF. Under these conditions (5 mM external Ca^{2+}), most of the inward current at negative potentials is carried through CRAC channels and is blocked reversibly by SKF. Although SKF decreases both CRAC and MIC components of inward current, the reduction of MIC current was complete and irreversible. Washout of SKF revealed CRAC current in isolation. A complementary approach to observe MIC current in isolation can be taken using Mg^{2+} as a selectively permeant ion (Fig. 11 B). In this experiment, with $NMDG^+$ substituted for Na^+, Mg^{2+} serves as the only external permeant ion; the MIC current develops as expected during dialysis and then is irreversibly reduced by exposure to SKF. These experiments illustrate that CRAC and MIC components are separable according to characteristic properties of run-down and ion permeation.

If the current remaining after run-down of the MIC current is indeed CRAC, then one would expect the

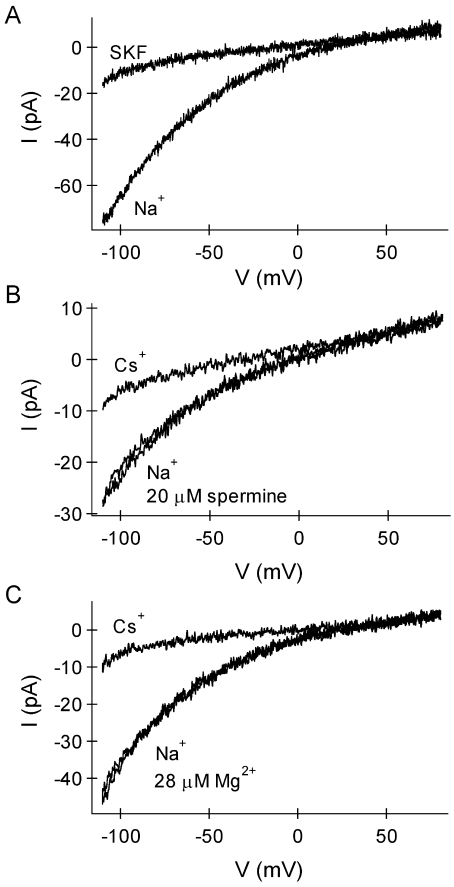

FIGURE 10. Pharmacological properties of monovalent CRAC current. CRAC current was allowed to develop in external Ca^{2+} and Na^+ current through CRAC channels was recorded in Na^+–HEDTA. The internal solution contained: 12 EGTA, and 6 (3 mM free) Mg^{2+}. (A) Effect of 20 μM SKF-96365 on Na^+ current through CRAC channels. SKF block was fully reversible. (B) I-V of Na^+ current through CRAC channels in the presence and absence of 20 μM spermine. (C) I-V of Na^+ current through CRAC channels in the presence and absence of 28 μM external Mg^{2+}, a free Mg^{2+} concentration that effectively blocks MIC current (Fig. 4 B). At the end of the experiment (B and C) external Na^+–HEDTA was substituted by Cs^+–HEDTA; the loss of inward current confirms that the monovalent current is through CRAC channels.

monovalent permeability to change depending on the time of recording. In Fig. 12, the current is shown developing in presence of 2 mM external Ca^{2+}. The external solution was subsequently changed to Na^+– and then Cs^+–HEDTA in order to record the corresponding monovalent current. Both Na^+ and Cs^+ show large current with linear I-V relationship (Fig. 12, A and D), as expected if most of the current is MIC. Furthermore, both Cs^+ and Na^+ currents continued to increase as additional MIC channels activate. Subsequent application of SKF caused irreversible run-down of Cs^+ current (Fig. 12, B and E, trace 5). At the end of the experiment, reexposure to Na^+–HEDTA solution revealed a significant increase in inward monovalent current (Fig. 12, B and E, trace 6); the remaining Na^+ current after run-down of MIC current showed the familiar inwardly rectifying I-V shape, unlike the linear I-V relationship in the same solution before MIC current ran down. This experiment demonstrates that the combined monovalent permeability switches from $Cs^+ \sim Na^+$ to $Na^+ >> Cs^+$ over the course of experiment, further confirming that two separate channels, with different permeability and I-V shape, carry the monovalent current. It also shows that the difference in selectivity of the monovalent currents recorded with high and low internal Mg^{2+} is not due to Mg^{2+} effects on the same channel, since the same internal solution is present throughout. Remarkably, CRAC current usually persists over extended periods of time (Fig. 8 A), long after MIC has completely disappeared. The fact that CRAC and MIC do not run down together can therefore be used for current separation.

DISCUSSION

CRAC channels are activated upon depletion of Ca^{2+} from the IP_3-sensitive intracellular store in Jurkat or RBL cells. Whole-cell and perforated-patch recordings have provided a biophysical characterization of these channels (Lewis and Cahalan, 1989; Hoth and Penner, 1992; Partiseti et al., 1994; for review see Parekh and Penner, 1997), but a detailed understanding of underlying molecular mechanisms remains elusive. We compared the properties of cation currents that develop during passive store depletion with and without internal Mg^{2+} using a wide range of membrane potentials, different ionic conditions, and several blocking agents. Table I serves as a guide for experimental manipulations that can isolate and distinguish CRAC and MIC channels by differences in ion permeation, kinetics of development and run-down, and pharmacological sensitivities. Differences in ion permeation and channel pharmacology argue in favor of two separate channels, but multiple effects of Mg^{2+} removal on a single channel type are difficult to rule out. In addition, we show that CRAC and MIC components can be isolated kinetically by exploiting the selective run-down of MIC current; this provides an opportunity to compare and contrast CRAC and MIC currents under identical ionic conditions. Our results show that CRAC currents, investigated in isolation without internal Mg^{2+} after MIC current run-down, retain their normal properties, including strong selectivity for Ca^{2+} over Mg^{2+} and Na^+ over $Cs^+$and reversible block by SKF-96365 but not spermine or Mg^{2+}. The simplest interpretation of the available data is that CRAC and MIC currents represent two distinct channel types.

Comparison of MIC and CRAC Currents

Both MIC and CRAC are Ca^{2+}-permeable channels that activate gradually after whole-cell recording mode is established with Ca^{2+} chelators in the pipette. Inward currents are comparable in size and I-V shape at hyper-

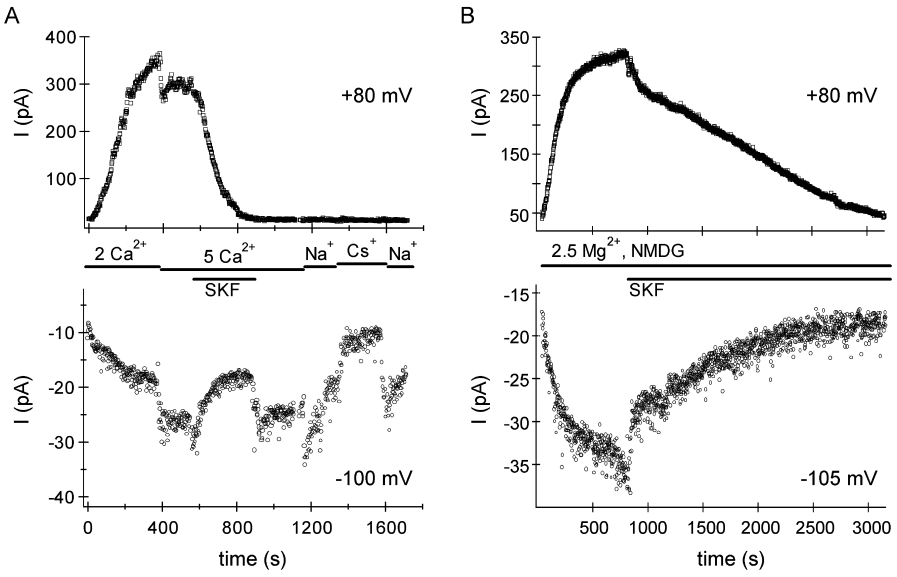

FIGURE 11. Separation of MIC and CRAC currents using SKF-induced run-down of MIC with low Mg^{2+} inside. (A) Development of MIC and CRAC currents in the same cell. External solution was 2 mM Ca^{2+} switched to 5 mM to increase inward current. SKF-96365 application caused slow reduction of both the outward and inward currents. The outward current ran down completely in presence of SKF. Removal of SKF did not increase outward current but reversed the inhibition of the inward current. The remaining inward current in 5 mM Ca^{2+} after washout of SKF is CRAC current. External solution is switched from Na^+– to Cs^+–HEDTA. Internal solution contained 12 EGTA, 0.5 mM Mg^{2+}. (B) MIC current isolated by use of 2.5 mM external Mg^{2+}. SKF caused irreversible run-down of both inward and outward currents, leaving no residual CRAC current in the absence of external Ca^{2+}.

polarized potentials (10–35 pA). Like voltage-gated Ca^{2+} channels, both MIC and CRAC conduct monovalent cations when external divalents are omitted. Although potent and selective blockers are not yet available, pharmacological sensitivities show some similarities. Micromolar concentrations of SKF-96365 inhibit both currents in a voltage-independent manner, albeit with different kinetics of block. Lanthanides also block both MIC and CRAC. The present study emphasizes the major differences in ion permeation, regulation,

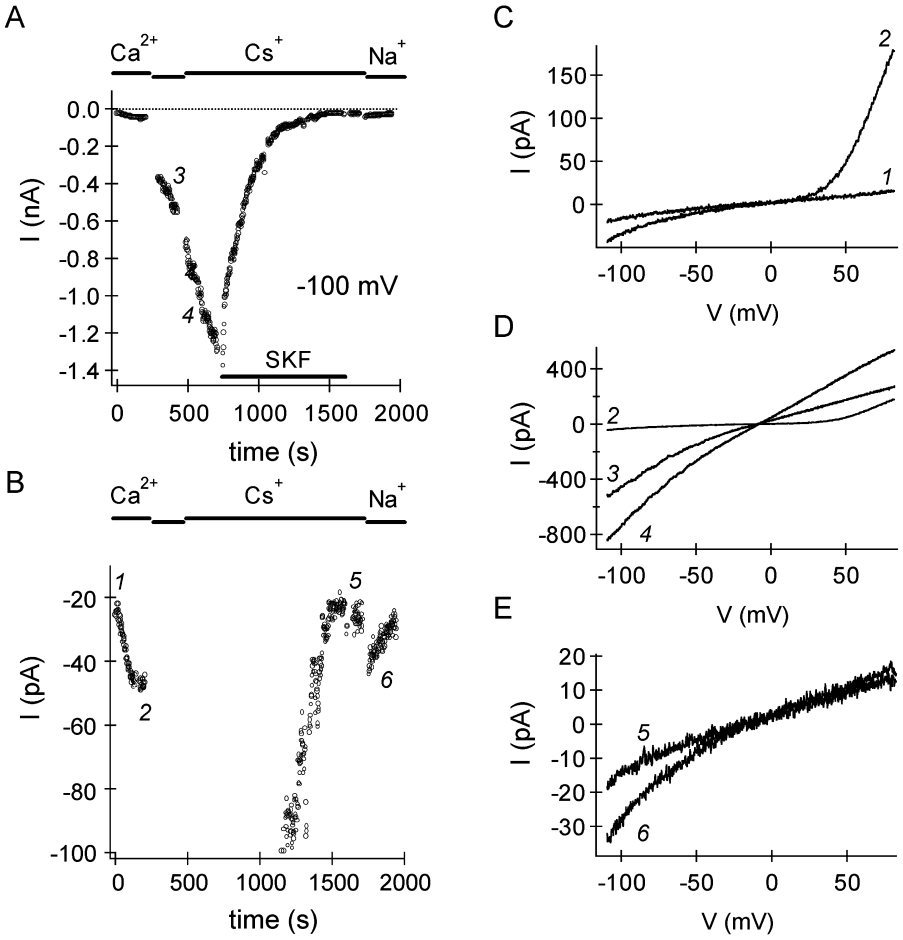

FIGURE 12. Change in the monovalent current selectivity after MIC current run-down induced by SKF-96365. Internal solution was 12 mM EGTA, 0.5 mM (280 μM free) Mg^{2+}. (A) Time course of CRAC and MIC currents. SKF-96365 (20 μM) is applied in Cs^+ and the MIC current was allowed to run down completely. After washout of SKF, reintroduction of Na^+ shows an increased inward current. (B) Same as A with expanded current scale. (C and D) I-V of the combined current before MIC current run-down in 2 mM Ca^{2+} (C, same trace at different scale in D) and Na^+– and Cs^+–HEDTA (D). (E) I-V of monovalent CRAC in Na^+– and Cs^+–HEDTA after MIC run-down.

TABLE I

Properties of CRAC and MIC Channels in RBL Cells

	CRAC	MIC
Permeability to external Mg^{2+}	not permeable	permeable[a]
Monovalent cation permeability	$Na^+ >> Cs^+$	$Cs^+ \geq Na$
Reversal potential (divalents)	>40 mV	~0 mV[a]
Reversal potential (Na^+)	>25 mV	~0 mV[a]
Unitary Na^+ conductance	0.2 pS[b]	40 pS
Rectification of		
divalent current	strong inward	strong outward[a]
monovalent current	strong inward	semilinear[a]
Mg^{2+} dependent rectification	No	No
Development time	50–200 s	100–500 s
Run-down with low internal Mg^{2+}	infrequent	frequent
Store dependence	Yes	No[a]
Inhibition by internal Mg^{2+}	No	Yes, mM[a]
Inhibition by external Mg^{2+}	Yes, high mM	Yes, low mM
Inactivation of Na^+ current	Yes	No[a]
Sensitivity to SKF-96365		
divalent and monovalent	reversible block	irreversible inhibition
External spermine block		
monovalent	No	Yes, low μM

[a]Designates properties that are similar to TRPM7 (derived from Nadler et al., 2001; Runnels et al., 2001).

[b]Derived from Prakriya and Lewis (2002).

and block between these two currents, as summarized in Table I.

CRAC channels are permeable to Ca^{2+}, Ba^{2+}, and Sr^{2+}, but not Mg^{2+} ions (Zweifach and Lewis, 1993; Fierro and Parekh, 2000; Fig. 8), and readily admit Na^+, Li^+, K^+, and Rb^+, but not Cs^+ ions when external divalent ions are removed (Hoth and Penner, 1993; Lepple-Wienhues and Cahalan, 1996; Fig. 11). On the other hand, MIC channels are permeable to Mg^{2+} and Cs^+ (Nadler et al., 2001; Figs. 1 and 2). Although Mg^{2+} permeability is unusual it is not without precedent among nonselective cation channels (e.g., Dani and Eisenman, 1987). At physiological levels of external Ca^{2+} and Na^+, the reversal potentials were near 0 mV for MIC current, indicating a nonselective cation conductance, and were clearly >40 mV for CRAC current consistent with a highly Ca^{2+}-selective current. In Jurkat and human T lymphocytes and in RBL cells, the macroscopic monovalent current that develops with low internal Mg^{2+} consists of the summed activity of tens to hundreds of 40-pS channels (Kerschbaum and Cahalan, 1999; Fomina et al., 2000; Braun et al., 2001); these represent activity of MIC channels. Single CRAC currents still have not been detected. From analysis of current fluctuations, variance and mean current measurements provide an estimate in the low fS range with Ca^{2+} as the permeant ion species, and from 2.8 to 0.2 pS with Na^+ as the permeant ion (Lepple-Wienhues and Cahalan, 1996; Prakriya and Lewis, 2002). In retrospect, the former estimate may have included a contribution from a small fraction of MIC channels with a much larger single-channel conductance of ~40 pS (Kerschbaum and Cahalan, 1999).

MIC and CRAC channels showed marked differences in I-V characteristics; MIC is a strongly outward-rectifying current, increasing steeply in magnitude >40 mV, whereas CRAC is a an inwardly rectifying current that reveals no detectable outward current beyond the same potential. In the absence of external divalents, CRAC current remained inwardly rectifying (Fig. 8), whereas MIC current lost outward rectification and became nearly linear (Fig. 3). With micromolar internal free Mg^{2+} (recorded after MIC has run down), CRAC still demonstrated inward rectification (Fig. 12). Differences in CRAC and MIC I-V shapes appear to be intrinsic to each respective channel. During channel activation, both MIC and CRAC currents increased uniformly at all potentials, and I-V shapes were unaffected by widely varying levels of internal Mg^{2+} (Figs. 3 and 9).

CRAC and MIC currents also exhibited distinct sensitivities to two different pharmacological agents, spermine and SKF-96365. In the absence of external divalent cations, MIC currents (carried by Cs^+ or Na^+) were reversibly blocked at micromolar concentrations by external Mg^{2+} or by external spermine, whereas monovalent CRAC was unaffected. Inhibition by internal Mg^{2+} was voltage- and time-independent and clearly different from the voltage-dependent block produced by external Mg^{2+} or spermine (Figs. 4 and 6). Both Mg^{2+} and spermine block were strongly voltage-dependent with considerable relief of block observed at positive potentials and partial relief at extremely negative potentials, consistent with punch-through seen by several pore blockers in other channel types. 20 μM SKF-96365 inhibited divalent or monovalent CRAC currents rapidly and reversibly, with millimolar internal Mg^{2+} or with low internal Mg^{2+} after run-down of MIC (Figs. 10 and 11). In contrast, SKF reduced the MIC current slowly over several minutes, and this reduction in current amplitude (seen uniformly at all potentials) was irreversible (Fig. 7). The effect of SKF was complex and may imply that a loss of cytoplasmic factors from the cytoplasm is required for its expression. Preincubation with SKF did not noticeably alter development of MIC current. Moreover, SKF did not affect the MIC current when applied early during the recording. In the absence of an exact mechanism, we hypothesize that SKF may facilitate MIC current run-down.

What Are the Mechanisms of Activation and Run-down of MIC Current?

When internal Mg^{2+} is reduced by whole-cell dialysis, MIC current develops gradually over several minutes, reaching a maximal amplitude ~10 min after break-in. Both the time course of MIC current development and the maximal current amplitudes varied from cell to cell. MIC current developed even when internal EGTA

was lowered from 12 to 1 mM and with levels of free Ca^{2+} that would be expected to sustain Ca^{2+}-store content, suggesting that passive depletion of stores was not important for activation. Pretreatment of the cells with 1 μM thapsigargin (8 min) also did not change activation of MIC current (unpublished data). Furthermore, addition of 10 or 100 μM internal free Ca^{2+} while omitting internal Ca^{2+} chelators also did not prevent MIC current from activating (unpublished data). Thus, we find no evidence that MIC is a store-operated conductance in RBL cells. A small fraction of cells exhibited significant MIC current immediately upon break-in. Inclusion of millimolar concentrations of free Mg^{2+} in the pipette reduced this preactivated component of MIC current with a time course slower than expected for free Mg^{2+} diffusion (Fig. 4 A), suggesting a mechanism more complex than a direct channel–Mg^{2+} interaction. The mechanism for MIC-current activation may involve the removal of tonic inhibition by an endogenous molecule, since MIC current is not increased during prolonged perforated-patch recording (unpublished data). It is notable that in other cell types cation conductances that are blocked by external divalent ions also develop over a time course of minutes and are not store-dependent (e.g., Mubagwa et al., 1997).

MIC and IRK current develop and run down in parallel (Fig. 5 A), suggesting a common mechanism of regulation. The reasons for IRK increase after break-in remain unknown at present. IRK run-down is thought to be mediated by PIP_2 depletion in the membrane (Hilgemann and Ball, 1996; Huang et al., 1998; Rohacs et al., 1999). IRK current can be reactivated by specific PIP_2 isomers, is blocked by PIP_2 antibodies, and is reversibly inhibited by agonist stimulation that activates the PLC pathway (Jones, 1996). Recently, PIP_2 has been shown to be a required cofactor for TRPM7 channels (Runnels et al., 2002). Depletion of PIP_2 may be a mechanism for the nearly synchronous run-down of both IRK and MIC currents.

Comparison of MIC and CRAC to Cloned Channels

The I-V characteristic of the native MIC current shows a marked similarity to the cloned TRPM7 channel (Nadler et al., 2001; Runnels et al., 2001; Yamaguchi et al., 2001), as noted previously (Hermosura et al., 2002). Like MIC, TRPM7 current is inhibited by internal Mg^{2+} or Mg^{2+} nucleotides at millimolar concentrations and is present in a wide variety of cells, including RBL cells. Heterologously expressed TRPM7 conducts both Ca^{2+} and Mg^{2+} (Nadler et al., 2001) and Cs^+ and Na^+ in the absence of external divalent ions (unpublished data) and reverses close to 0 mV. It is likely that the current described previously in Jurkat and human T cells (Kerschbaum and Cahalan, 1998, 1999; Fomina et al., 2000) represents the TRPM7 channel.

Monovalent cation channels that lack voltage-dependent gating are revealed by removal of external divalent cations in a wide variety of cell types, including amphibian epithelial membranes (Van Driessche et al., 1993), chick embryo ectoderm (Sabovcik et al., 1996), *Xenopus* oocytes (Arellano et al., 1995), cardiac myocytes (Mubagwa et al., 1997; Bosteels et al., 1999), smooth muscle (Bae et al., 1999), hippocampal neurons (Xiong and MacDonald, 1999). Most of these channels have also been shown to conduct various divalent cations (Ca^{2+}, Ba^{2+}, Sr^{2+}) in the inward direction. Divalent currents through these channels are usually much smaller than monovalent currents at the same voltage, even when divalent concentrations are in the millimolar range. All of the above-mentioned conductances display weak selectivity among K^+, Na^+, Cs^+, Rb^+, and other small monovalent cations when external divalent ions are removed. Many of these native currents may represent activity of TRPM7 or related TRP channels.

Another member of the TRP family of ion channels, TRPV6 (also known as CaT1 or ECaC2) is a Ca^{2+}-permeable channel that has been proposed to be store operated and to underlie native CRAC currents (Yue et al., 2001). Some important properties of CaT1, such as Na^+/Cs^+ permeability, effects of 2-APB, and voltage-dependent gating, are, however, different from those of native CRAC currents (Voets et al., 2001). Effects of internal Mg^{2+} (or lack therein) on rectification can be considered a useful characteristic for testing candidate CRAC channel clones that express inwardly rectifying channels.

Mechanisms of Inward Rectification – CRAC and other Channels

Several channels are known to have inwardly rectifying I-V relationships. Internal Mg^{2+} can produce inward rectification in inwardly rectifying K^+ channels, nicotinic acetylcholine receptor channels, L-type Ca^{2+} channels, and voltage-gated Na^+ channels by blocking the open channel pore from inside at depolarized membrane potentials (Armstrong, 1969; Vandenberg, 1987; Matsuda et al., 1987; Pusch, 1990; Ifune and Steinbach, 1992; Kuo and Hess, 1993; Nichols et al., 1994; Forster and Bertrand, 1995). Here, we demonstrate that the inward rectification of CRAC channels is an intrinsic channel property and not a consequence of a voltage-dependent block of the channel by internal Mg^{2+}, as previously suggested (Kerschbaum and Cahalan, 1998). Mg^{2+} block as a mechanism for inward rectification of the CRAC channel was ruled out by varying internal Mg^{2+} systematically from micromolar to millimolar levels with no observed change in the characteristic shape of the I-V relation. In addition to open channel block by internal Mg^{2+}, another mechanism for rectification appears to be the voltage-dependent block of channels by internal spermine and other

polyamines, organic positively charged molecules present in vertebrate cells. This mechanism of rectification has been demonstrated in various channel types, such as inwardly rectifying K^+ channels, AMPA glutamate receptors (for review see Williams, 1997), and nAChRs (Haghighi and Cooper, 2000), However, inward rectification of CRAC channels is unlikely to be caused by another intracellular blocking ion because prolonged recording (30–60 min) in whole-cell mode does not alter the inward rectification of CRAC current. Thus, we propose that the mechanism of inward rectification of CRAC channels is intrinsic to the protein. TRPV6 (CaT1) and TRPV5 (CaT2) display pronounced inward rectification and a high degree of Ca^{2+} selectivity. The mechanism for rectification is unexplored in these channels. However, it is unlikely that internal Mg^{2+} mediates it, as strong inward rectification of CaT1 persists when Mg^{2+} is in the micromolar range or is entirely omitted from intracellular solution (unpublished data; Vennekens et al., 2000; Voets et al., 2001; Yue et al., 2001). Importantly, CaT1 current carried by monovalent cations also maintains its inward rectification in the absence of internal Mg^{2+} (Yue et al., 2001, Fig. 2). Thus, TRPV5 and 6 serve as examples of Ca^{2+}-selective channels that display strong inward rectification independent of internal Mg^{2+} block.

Physiological Roles

Ca^{2+} influx through CRAC channels is required to generate Ca^{2+} signaling, gene expression, and cell proliferation in T lymphocytes (for review see Lewis, 2001), but unfortunately mechanistic and molecular aspects of these channels remain unclear. It appears that we know even less about these channels than previously thought (Kerschbaum and Cahalan, 1999), since the single channels formerly attributed to CRAC are instead likely to be TRPM7 channels that coactivate when passive Ca^{2+}-store depletion is combined with low internal Mg^{2+}. Our results complement recent work and provide a cautionary note on current separation (Hermosura et al., 2002; Prakriya and Lewis, 2002). Noise estimates for single-channel CRAC conductance (Zweifach and Lewis, 1993; Prakriya and Lewis, 2002) suggest that CRAC channels are abundantly expressed in Jurkat T cells, from 5,000 to 10,000 functional channels per cell. Functional expression of MIC channels (previously identified as CRAC) is up-regulated by an order of magnitude when human T cells are stimulated to proliferate (Fomina et al., 2000), in parallel with dramatic changes in expression levels of voltage-gated K^+ channels (Kv1.3) and Ca^{2+}-activated K^+ channels (IKCa1) (for review see Cahalan et al., 2001). It will be important to assess expression levels of CRAC channels in normal T cells, both resting and in varying states of activation. Selective blockers of the sort that have been developed for lymphocyte K^+ channels (Chandy et al., 2001) are not yet available for CRAC or MIC channels. Molecular and pharmacological tools will be important to establish functional roles of CRAC and MIC channels in the immune system.

We thank Lu Forrest for technical assistance and Reinhold Penner and Richard Lewis for sharing data before publication. We are grateful to George Chandy for helpful comments on the manuscript.

This paper was supported by National Institutes of Health grant #NS-14609.

Submitted: 27 March 2002
Revised: 13 June 2002
Accepted: 14 June 2002

REFERENCES

Almers, W., and E.W. McCleskey. 1984. Non-selective conductance in calcium channels of frog muscle: calcium selectivity in a single-file pore. *J. Physiol.* 353:585–608.

Arellano, R.O., R.M. Woodward, and R. Miledi. 1995. A monovalent cation conductance that is blocked by extracellular divalent cations in *Xenopus* oocytes. *J. Physiol.* 484:593–604.

Armstrong, C.M. 1969. Inactivation of the potassium conductance and related phenomena caused by quaternary ammonium ion injection in squid axons. *J. Gen. Physiol.* 54:553–575.

Bae, Y.M., M.K. Park, S.H. Lee, W.K. Ho, and Y.E. Earm. 1999. Contribution of Ca^{2+}-activated K^+ channels and non-selective cation channels to membrane potential of pulmonary arterial smooth muscle cells of the rabbit. *J. Physiol.* 514:747–758.

Bosteels, S., P. Matejovic, W. Flameng, and K. Mubagwa. 1999. Sodium influx via a non-selective pathway activated by the removal of extracellular divalent cations: possible role in the calcium paradox. *Cardiovasc. Res.* 43:417–425.

Braun, F.J., L.M. Broad, D.L. Armstrong, and J.W.J. Putney. 2001. Stable activation of single Ca^{2+} release-activated Ca^{2+} channels in divalent cation-free solutions. *J. Biol. Chem.* 276:1063–1070.

Cahalan, M.D., H. Wulff, and K.G. Chandy. 2001. Molecular properties and physiological roles of ion channels in T lymphocytes. *J. Clin. Immunol.* 21:235–252.

Chandy, K.G., M.D. Cahalan, M. Pennington, R.S. Norton, H. Wulff, and G.A. Gutman. 2001. Potassium channels in T lymphocytes: toxins to therapeutic immunosuppressants. *Toxicon.* 39:1269–1276.

Chung, S.C., T.V. McDonald, and P. Gardner. 1994. Inhibition by SK&F 96365 of Ca^{2+} current, IL-2 production and activation in T lymphocytes. *Br. J. Pharmacol.* 113:861–868.

Dani, J.A., and G. Eisenman. 1987. Monovalent and divalent cation permeation in acetylcholine receptor channels. Ion transport related to structure. *J. Gen. Physiol.* 89:959–983.

Fierro, L., and A.B. Parekh. 2000. Substantial depletion of the intracellular Ca^{2+} stores is required for macroscopic activation of the Ca^{2+} release-activated Ca^{2+} current in rat basophilic leukemia cells. *J. Physiol.* 522:247–257.

Fomina, A.F., C.M. Fanger, J.A. Kozak, and M.D. Cahalan. 2000. Single channel properties and regulated expression of Ca^{2+} release-activated Ca^{2+} (CRAC) channels in human T cells. *J. Cell Biol.* 150:1435–1444.

Forster, I., and D. Bertrand. 1995. Inward rectification of neuronal nicotinic acetylcholine receptors investigated by using the homomeric alpha 7 receptor. *Proc. R. Soc. Lond. B Biol. Sci.* 260:139–148.

Haghighi, A.P., and E. Cooper. 2000. A molecular link between inward rectification and calcium permeability of neuronal nicotinic acetylcholine alpha3beta4 and alpha 4beta2 receptors. *J. Neurosci.* 20:529–541.

Hermosura, M.C., M.K. Monteilh-Zoller, A.M. Scharenberg, R. Penner, and A. Fleig. 2002. Dissociation of the store-operated cal-

cium current I_{CRAC} and the Mg^{2+}-nucleotide-regulated metal ion current MagNuM. *J. Physiol.* 539:445–458.

Hess, P., and R.W. Tsien. 1984. Mechanism of ion permeation through calcium channels. *Nature.* 309:453–456.

Hilgemann, D.W., and R. Ball. 1996. Regulation of cardiac Na^+,Ca^{2+} exchange and KATP potassium channels by PIP_2. *Science.* 273:956–959.

Hoth, M., and R. Penner. 1992. Depletion of intracellular calcium stores activates a calcium current in mast cells. *Nature.* 355:353–356.

Hoth, M., and R. Penner. 1993. Calcium release-activated calcium current in rat mast cells. *J. Physiol.* 465:359–386.

Huang, C.L., S. Feng, and D.W. Hilgemann. 1998. Direct activation of inward rectifier potassium channels by PIP_2 and its stabilization by Gβγ. *Nature.* 391:803–806.

Huang, C.J., and E. Moczydlowski. 2001. Cytoplasmic polyamines as permeant blockers and modulators of the voltage-gated sodium channel. *Biophys. J.* 80:1262–1279.

Ifune, C.K., and J.H. Steinbach. 1992. Inward rectification of acetylcholine-elicited currents in rat phaeochromocytoma cells. *J. Physiol.* 457:143–165.

Jones, S.V. 1996. Modulation of the inwardly rectifying potassium channel IRK by the m1 muscarinic receptor. *Mol. Pharmacol.* 49: 662–667.

Kerschbaum, H.H., and M.D. Cahalan. 1998. Monovalent permeability, rectification, and ionic block of store-operated calcium channels in Jurkat T lymphocytes. *J. Gen. Physiol.* 111:521–537.

Kerschbaum, H.H., and M.D. Cahalan. 1999. Single-channel recording of a store-operated Ca^{2+} channel in Jurkat T lymphocytes. *Science.* 283:836–839.

Kozak, J.A., and M.D. Cahalan. 2001. Pharmacological properties of the 40 pS monovalent current in T cells and RBL cells. *Soc. Neurosci. Abstr.* 27. (Abstr.)

Kozak, J.A., and M.D. Cahalan. 2002. CRAC and QUAC in RBL cells. *Biophys. J.* 82. (Abstr.)

Kuo, C.C., and P. Hess. 1993. Block of the L-type Ca^{2+} channel pore by external and internal Mg^{2+} in rat phaeochromocytoma cells. *J. Physiol.* 466:683–706.

Lepple-Wienhues, A., and M.D. Cahalan. 1996. Conductance and permeation of monovalent cations through depletion-activated Ca^{2+} channels (I_{CRAC}) in Jurkat T cells. *Biophys. J.* 71:787–794.

Lewis, R.S. 2001. Calcium signaling mechanisms in T lymphocytes. *Annu. Rev. Immunol.* 19:497–521.

Lewis, R.S., and M.D. Cahalan. 1989. Mitogen-induced oscillations of cytosolic Ca^{2+} and transmembrane Ca^{2+} current in human leukemic T cells. *Cell Regul.* 1:99–112.

Lu, Z., and L. Ding. 1999. Blockade of a retinal cGMP-gated channel by polyamines. *J. Gen. Physiol.* 113:35–43.

Matsuda, H., A. Saigusa, and H. Irisawa. 1987. Ohmic conductance through the inwardly rectifying K channel and blocking by internal Mg^{2+}. *Nature.* 325:156–159.

McCloskey, M.A., and M.D. Cahalan. 1990. G protein control of potassium channel activity in a mast cell line. *J. Gen. Physiol.* 95:205–227.

Merritt, J.E., W.P. Armstrong, C.D. Benham, T.J. Hallam, R. Jacob, A. Jaxa-Chamiec, B.K. Leigh, S.A. McCarthy, K.E. Moores, and T.J. Rink. 1990. SK&F 96365, a novel inhibitor of receptor-mediated calcium entry. *Biochem. J.* 271:515–522.

Mubagwa, K., M. Stengl, and W. Flameng. 1997. Extracellular divalent cations block a cation non-selective conductance unrelated to calcium channels in rat cardiac muscle. *J. Physiol.* 502:235–247.

Nadler, M.J., M.C. Hermosura, K. Inabe, A.L. Perraud, Q. Zhu, A.J. Stokes, T. Kurosaki, J.P. Kinet, R. Penner, A.M. Scharenberg, and A. Fleig. 2001. LTRPC7 is a Mg.ATP-regulated divalent cation channel required for cell viability. *Nature.* 411:590–595.

Nichols, C.G., K. Ho, and S. Hebert. 1994. Mg^{2+}-dependent inward rectification of ROMK1 potassium channels expressed in *Xenopus* oocytes. *J. Physiol.* 476:399–409.

Parekh, A.B., and R. Penner. 1997. Store depletion and calcium influx. *Physiol. Rev.* 77:901–930.

Partiseti, M., F. Le Deist, C. Hivroz, A. Fischer, H. Korn, and D. Choquet. 1994. The calcium current activated by T cell receptor and store depletion in human lymphocytes is absent in a primary immunodeficiency. *J. Biol. Chem.* 269:32327–32335.

Prakriya, M., and R.S. Lewis. 2002. Separation and characterization of currents through store-operated CRAC channels and Mg^{2+}-inhibited cation (MIC) channels. *J. Gen. Physiol.* 119:487–508.

Premack, B.A., T.V. McDonald, and P. Gardner. 1994. Activation of Ca^{2+} current in Jurkat T cells following the depletion of Ca^{2+} stores by microsomal Ca^{2+}-ATPase inhibitors. *J. Immunol.* 152:5226–5240.

Pusch, M. 1990. Open-channel block of Na^+ channels by intracellular Mg^{2+}. *Eur. J. Biophys.* 18:317–326.

Pusch, M., and E. Neher. 1988. Rates of diffusional exchange between small cells and a measuring patch pipette. *Pflugers Arch.* 411:204–211.

Rohacs, T., J. Chen, G.D. Prestwich, and D.E. Logothetis. 1999. Distinct specificities of inwardly rectifying K^+ channels for phosphoinositides. *J. Biol. Chem.* 274:36065–36072.

Runnels, L.W., L. Yue, and D.E. Clapham. 2001. TRP-PLIK, a bifunctional protein with kinase and ion channel activities. *Science.* 291:1043–1047.

Runnels, L.W., L. Yue, and D.E. Clapham. 2002. The TRPM7 channel is inactivated by PIP_2 hydrolysis. *Nat. Cell Biol.* 5:329–336.

Sabovcik, R., P. Kucera, and B. Prod'hom. 1996. Characterization of a whole-cell Ca^{2+}-blockable monovalent cation current in isolated ectodermal cells of chick embryo. *Pflugers Arch.* 431:599–607.

Siraganian, R.P., A. McGivney, E.L. Barsumian, F.T. Crews, F. Hirata, and J. Axelrod. 1982. Variants of the rat basophilic leukemia cell line for the study of histamine release. *Fed. Proc.* 41:30–34.

Van Driessche, W., L. Desmedt, P. De Smet, and J. Simaels. 1993. Poorly selective cation channels in apical membranes of epithelia. *EXS.* 66:225–245.

Vandenberg, C.A. 1987. Inward rectification of a potassium channel in cardiac ventricular cells depends on internal magnesium ions. *Proc. Natl. Acad. Sci. USA.* 84:2560–2564.

Vennekens, R., J.G. Hoenderop, J. Prenen, M. Stuiver, P.H. Willems, G. Droogmans, B. Nilius, and R.J. Bindels. 2000. Permeation and gating properties of the novel epithelial Ca^{2+} channel. *J. Biol. Chem.* 275:3963–3969.

Voets, T., A. Fleig, R. Vennekens, H. Watanabe, J.G. Hoenderop, R.J. Bindels, G. Droogmans, R. Penner, and B. Nilius. 2001. CaT1 and the calcium-release activated calcium channel manifest distinct pore properties. *J. Biol. Chem.* 276:47767–47770.

Williams, K. 1997. Modulation and block of ion channels: a new biology of polyamines. *Cell. Signal.* 9:1–13.

Wischmeyer, E., K.U. Lentes, and A. Karschin. 1995. Physiological and molecular characterization of an IRK-type inward rectifier K+ channel in a tumour mast cell line. *Pflugers Arch.* 429:809–819.

Xiong, Z.G., and J.F. MacDonald. 1999. Sensing of extracellular calcium by neurones. *Can. J. Physiol. Pharmacol.* 77:715–721.

Yamaguchi, H., M. Matsushita, A.C. Nairn, and J. Kuriyan. 2001. Crystal structure of the atypical protein kinase domain of a TRP channel with phosphotransferase activity. *Mol. Cell.* 7:1047–1057.

Yue, L., J.B. Peng, M.A. Hediger, and D.E. Clapham. 2001. CAT1 manifests the pore properties of the calcium-release-activated calcium channel. *Nature.* 410:705–709.

Zweifach, A., and R.S. Lewis. 1993. Mitogen-regulated Ca^{2+} current of T lymphocytes is activated by depletion of intracellular Ca^{2+} stores. *Proc. Natl. Acad. Sci. USA.* 90:6295–6299.

Zweifach, A., and R.S. Lewis. 1996. Calcium-dependent potentiation of store-operated calcium channels in T lymphocytes. *J. Gen. Physiol.* 107:597–610.